

# Double-Diffusive Natural Convection Flows with Thermosolutal Symmetry in Porous Media in the Presence of the Soret–Dufour Effects

Eugen Magyari · Adrian Postelnicu

Received: 4 December 2010 / Accepted: 14 January 2011 / Published online: 5 February 2011  
© Springer Science+Business Media B.V. 2011

**Abstract** The double-diffusive natural convection past a vertical plate embedded in a fluid-saturated porous medium is considered in the boundary-layer and Boussinesq approximations. It is assumed that the Soret–Dufour cross-diffusion effects are significant. The heat and mass fluxes on the plate are prescribed as functions of the surface coordinate  $x$ . The general similarity reduction of the problem for power-law and exponential variation of the wall fluxes is given. In the case of thermosolutal symmetry, when the similar temperature and concentration fields become coincident, exact analytical as well as numerical solutions are reported and discussed in some detail. For the flows without thermosolutal symmetry, the final similarity equations have been solved numerically, by paying attention to the influence of the Soret and Dufour numbers on the departure from thermosolutal symmetry. The reported results focus on the wall temperatures and concentrations, whose reciprocals are Nusselt and Sherwood numbers, respectively.

**Keywords** Natural convection · Vertical surface · Double diffusion · Prescribed fluxes · Self-similarity · Thermosolutal symmetry · Cross-diffusion effects · Porous media

## 1 Introduction

Thermal diffusion, also called thermodiffusion or Soret effect, corresponds to species differentiation developing in an initial homogeneous mixture subjected to a temperature gradient (Soret 1980). The heat flux induced by a concentration gradient is called Dufour or diffusion-thermo effect. These effects are considered as second order phenomena, on the basis that they are of smaller order of magnitude than the effects described by Fourier's and Fick's

---

E. Magyari  
Departement Physik, Universität Basel, Klingelbergstr. 82, 4056 Basel, Switzerland

A. Postelnicu (✉)  
Department of Thermal Engineering and Fluid Mechanics, Transilvania University,  
500036 Brasov, Romania  
e-mail: adip@unitbv.ro

laws, but there are situations when they become significant. For instance, [Eckert and Drake \(1972\)](#) presented several cases of Dufour effect.

There is an obvious interest in including Dufour and Soret effects in the analysis of convective processes in both clear fluids and porous media. Restricting our considerations to porous media, let us refer further to the textbook by [Nield and Bejan \(2006\)](#) where some basic information are given on pages 42–44. According to the references quoted there,

- In most liquid mixtures, the Dufour effect is inoperative, but that this may not be the case in gases ([Platten and Legros 1984](#)). This fact was confirmed also by [Mojtabi and Charrier-Mojtabi \(2000\)](#), who found that in liquids the Dufour coefficient is an order of magnitude smaller than the Soret effect.
- A not encouraging conclusion was drawn by these later authors, [Mojtabi and Charrier-Mojtabi \(2000\)](#), in the sense that for saturated porous media, the phenomenon of cross-diffusion is complicated due to the interaction between the fluid and the porous matrix. This is the reason why accurate values of these coefficients are not (yet) available.
- In Chap. 9, “Double-diffusive convection”, the Soret effect is discussed in relation with the flow stability (pp. 374–376), in an extension of double-diffusive generalization of the Horton–Rogers–Lapwood problem. The formula (9.32) includes the Soret number in an analytic expression of the critical Rayleigh number, but no numerical values are given for this coefficient. Other references are given in that chapter, in relation with Soret and Dufour effects for porous layers and cavities. Note that this topic is currently under investigation, see for instance the very recent article by [Gaikwad et al. \(2009\)](#).

A very useful reference on thermodiffusion in porous media is that by [Saghir et al. \(2005\)](#), where it is presented an extensive literature review on the measurement techniques of the Soret coefficient and on the numerical works done in this area. The literature review shows that there are various techniques to measure the thermal diffusion coefficient, but one has to control strictly the experiments, in order to avoid the possible associated effect of thermal convection, “which is very difficult in ground conditions”. Consequently, they present a numerical procedure, developed to simulate this process. This procedure is demonstrated for polar and hydrocarbon mixtures, in cavities. In the final section of the chapter devoted to conclusions, the authors state: “Due to the difficulty in measuring thermal diffusion and mass diffusion coefficients accurately, it is hoped that numerical models could provide reliable results and thus reduce the burden of costly experiments”. One remarks to this end that no information is given concerning the Dufour effect.

Another direction to deal with these effects is to use the theory of thermodynamics of irreversible processes, as in [Li et al. \(2008\)](#) who considered a strongly endothermic chemical reaction system in a porous medium formed by spherical carbonate pellets in a reactor. However, orders of magnitude are given for these coefficients, in dimensional form, without physical justification and results are reported taking these coefficients as equal. For other references along this direction, the interested reader may also consult those ones presented by [Saghir et al. \(2005\)](#), reviewed above. In conclusion, it seems that various authors give more importance to the Soret effect in internal geometries, but for sake of space, we will skip here this discussion, because our interest in the present context is toward external heat and mass transfer convection driven by the Dufour and Soret effects.

Since the article by [Anghel et al. \(2000\)](#), an analytical progress in external convection with cross-diffusion (Dufour and Soret) effects was realized, by imposing certain rational values of these dimensionless coefficients. Lacking experimental data, it was a fair way to explore further this area of research. In an article by [Postelnicu \(2004\)](#), devoted to Dufour and Soret effects in free convection boundary-layer over a vertical isothermal surface embedded

in a porous medium, it was shown that these effects, coupled eventually with a magnetic field, appreciably influence the flow behavior. [Partha et al. \(2006\)](#) looked for the effect of double dispersion, Dufour and Soret effects in free convection heat and mass transfer in a non-Darcy electrically conducting fluid saturating a porous medium. In a related article, [Lakshmi Narayana and Murthy \(2007\)](#) studied the Soret and Dufour effects in a doubly stratified Darcy porous medium. Later on, [Lakshmi Narayana and Murthy \(2008\)](#) analyzed Soret and Dufour effects on free convection heat and mass transfer from a horizontal flat plate in a Darcy porous medium, and obtained similarity solutions in the case of constant wall temperature and concentration. More effects, besides Dufour and Soret, such as thermal dispersion and temperature-dependent viscosity have been introduced by [Afify \(2007a,b\)](#) in the analysis of non-Darcy MHD free convection past a vertical isothermal surface embedded in a porous medium.

Another contribution to the theme of Dufour and Soret effects in porous media can be found in the article by [Tsai and Huang \(2009a\)](#), where a Hiemenz flow through a porous medium is analyzed, by combining also various other effects, such as variable viscosity, heat source, radiation, and chemical reaction. The same authors studied in [Tsai and Huang \(2009b\)](#) the Dufour and Soret effects in a natural convection flow along a vertical plate configuration in a porous medium by prescribing the wall heat flux and the wall concentration.

Dufour and Soret effects in other external geometries have been also reported very recently: cone, by [Cheng \(2009\)](#), corrugated vertical surface, by [Rathish Kumar and Krishna Murthy \(2010\)](#). In these articles, constant wall temperature and concentration boundary conditions have been imposed. In a very recent article, [Postelnicu \(2010\)](#) dealt with Dufour and Soret effects on flow at a two-dimensional stagnation point in a fluid-saturated porous medium with suction/injection. Similarity solutions were obtained in that article, and besides the numerical solutions, asymptotic analytical solutions have been presented for the large suction rates.

The objective of the present article is to study simultaneous heat and mass transfer with cross-diffusion effects, by natural convection from a vertical surface embedded in a fluid-saturated Darcian porous medium, subject to prescribed heat and mass wall heat fluxes. We will adopt a systematic approach in searching for similarity solutions, aiming to find all the possible situations of this kind. We mention to this end that, aside from the present context, [Johnson and Cheng \(1978\)](#) presented a comprehensive listing of similarity solutions for free convection boundary-layers adjacent to flat plates in porous media, but without double diffusion with Dufour–Soret effects.

## 2 Basic Equations and Problem Formulation

We consider the double-diffusive natural convection past a vertical plate embedded in a porous medium saturated by an incompressible Newtonian fluid. The boundary-layer and the Boussinesq approximations are adopted and it is assumed that the Soret–Dufour cross-diffusion effects are significant. The  $x$ -coordinate is measured along the surface and the  $y$ -coordinate normal to it. The temperature of the ambient medium is  $T_\infty = \text{constant}$  and the wall heat flux is prescribed,  $q_w(x)$ . The flow contains a species A, which is slightly soluble in the fluid B, the wall mass flux of the species A being also prescribed,  $q_m(x)$ . The concentration of A in B far away from the plate is  $C_\infty$ . Further assumptions adopted in the following analysis are (i) the flow is laminar, steady, and two-dimensional, (ii) the porous medium is isotropic and homogeneous, (iii) the properties of the fluid and porous medium are constant except for the density variation required by the Boussinesq approximation, (iv) the fluid and the porous medium are in local thermodynamic equilibrium. Under these

conditions, the governing equations describing the conservation of mass and momentum can be written as follows

$$\frac{\partial u}{\partial x} + \frac{\partial v}{\partial y} = 0 \quad (1)$$

$$u = \frac{gK}{v} [\beta_T (T - T_\infty) + \beta_C (C - C_\infty)] \quad (2)$$

In a general form, the energy and concentration equations are expressed as

$$\frac{(\rho c)_m}{(\rho c)_f} \frac{\partial T}{\partial t} + \mathbf{V} \cdot \nabla T = \nabla \cdot (D_T \nabla T + D_{TC} \nabla C), \quad (3a)$$

$$\varphi \frac{\partial C}{\partial t} + \mathbf{V} \cdot \nabla C = \nabla \cdot (D_C \nabla C + D_{CT} \nabla T). \quad (4a)$$

(see [Nield and Bejan 2006](#)), where  $\varphi$  is the porosity of the medium,  $D_T = k_m / (\rho c)_f$  is the thermal diffusivity,  $D_C \equiv D_m$  is the mass diffusivity, while  $D_{TC}/D_T$  and  $D_{CT}/D_C$  may be considered as Dufour and Soret coefficients (numbers) of the porous medium. In recent years, basically in all articles dealing with this subject, the previous equations for the case of steady flows were used in the form

$$u \frac{\partial T}{\partial x} + v \frac{\partial T}{\partial y} = \alpha_m \frac{\partial^2 T}{\partial y^2} + \frac{D_m}{C_s} \frac{k_T}{C_p} \frac{\partial^2 C}{\partial y^2} \quad (3b)$$

$$u \frac{\partial C}{\partial x} + v \frac{\partial C}{\partial y} = D_m \frac{\partial^2 C}{\partial y^2} + \frac{D_m k_T}{T_m} \frac{\partial^2 T}{\partial y^2} \quad (4b)$$

where  $\alpha_m$  is the thermal diffusivity.  $C_p$  and  $C_s$  are the specific heat at constant pressure and concentration susceptibility and  $k_T$  is the thermal diffusion ratio. It seems that this form originates from an article by [Kafoussias and Williams \(1995\)](#), where Dufour and Soret effects have been considered in a free convection boundary-layer past a vertical plate in a viscous fluid.

The boundary conditions assumed in the present study are

$$v = 0, \quad -k \frac{\partial T}{\partial y} = q_w(x), \quad -D_m \frac{\partial C}{\partial y} = q_m(x) \text{ on } y = 0, \quad (5)$$

$$T \rightarrow T_\infty, \quad C \rightarrow C_\infty \text{ as } y \rightarrow \infty$$

where  $q_w(x)$  and  $q_m(x)$  denote the prescribed heat and mass flux distributions along the wall, respectively. The main goal of the article is (i) to give the similarity reduction of the boundary value problem when the prescribed fluxes are power-law or exponential functions of the plate coordinate  $x$ , and (ii) to discuss the cases of thermosolutal symmetry (when the similar temperature and concentration fields become coincident) in some detail.

### 3 Self-Similar Flows

#### 3.1 General Similarity Transformations

Introducing the stream function  $\psi$  by the usual definition  $u = \partial \psi / \partial y$ ,  $v = -\partial \psi / \partial x$ , the dimensionless coordinates  $X = x/l$ ,  $Y = y/l$  where  $l$  is a reference length, as well as the similarity transformations

$$\psi = \alpha_m A(X) f(\eta), \quad \eta = B(X) Y, \quad (6)$$

$$T = T_\infty + G(X) \theta(\eta), \quad C = C_\infty + H(X) \phi(\eta) \quad (7)$$

the velocity field becomes

$$u = u_0 A(X) B(X) f'(\eta), \quad (8)$$

$$v = -u_0 \left[ \dot{A}(X) f(\eta) + \frac{A(X) \dot{B}(X)}{B(X)} \eta f'(\eta) \right]$$

In the above equations,  $u_0 = \alpha_m / l$  is a reference velocity,  $A$  and  $B$  some, yet unknown, dimensionless functions of  $X$ ,  $\theta$ , and  $\phi$  stand for the dimensionless temperature and concentration fields, respectively. The primes denote differentiation with respect to similarity independent variable  $\eta$  and the dot with respect to  $X$ . The dimensional functions  $G(X)$  and  $H(X)$ , that have dimensions as  $[G] = [T]$ ,  $[H] = [C]$ , are related to the (unknown) temperature and concentration distributions  $T(x, 0) \equiv T_w(x)$  and  $C(x, 0) \equiv C_w(x)$  by the relationships

$$T_w(x) = T_\infty + G(X) \theta_0, \quad C_w(x) = C_\infty + H(X) \phi_0 \quad (9)$$

where  $\theta_0 = \theta(0)$  and  $\phi_0 = \phi(0)$ .

Bearing in mind Eqs. 7 and 8, the wall conditions (5) result in

$$\begin{aligned} f(0) &= 0, \\ q_w(x) &= -\frac{k}{l} G(X) B(X) \theta'(0), \\ q_m(x) &= -\frac{D_m}{l} H(X) B(X) \phi'(0) \end{aligned} \quad (10)$$

Imposing

$$\theta'(0) = -1, \quad \phi'(0) = -1 \quad (11)$$

one obtains for the functions  $B$ ,  $G$ , and  $H$ , the relationships

$$G(X) = \frac{l}{k} \frac{q_w(x)}{B(X)}, \quad H(X) = \frac{l}{D_m} \frac{q_m(x)}{B(X)} \quad (12)$$

Equations 7 and the asymptotic condition (5) require

$$\theta(\infty) = 0, \quad \phi(\infty) = 0 \quad (13)$$

Under the transformations (6) and (7) and on account of Eqs. 12, Eq. 2 becomes

$$f' = \frac{g \beta_T K l}{\nu \alpha_m} \frac{G}{AB} \left( \theta + \frac{\beta_C k}{\beta_T D_m} \frac{q_m(x)}{q_w(x)} \phi \right) \quad (14)$$

This equation shows that the similarity reduction of Eq. 2 is only possible when the fluxes  $q_w(x)$  and  $q_m(x)$  are of the form

$$q_w(x) = w q(X) \quad \text{and} \quad q_m(x) = m q(X) \quad (15)$$

where  $w$  and  $m$  are some dimensional constants and  $q(X)$  some positive definite dimensionless function of  $X$ . At the same time, it is necessary that the factor in front of the bracket expression (14) becomes a constant. Without any restriction of generality, one may require

$$\frac{g K l}{\nu \alpha_m} \frac{\beta_T G}{AB} = 1 \quad (16)$$

Thus, Eq. 14 becomes

$$f' = \theta + N\phi \quad (17)$$

and implies

$$f(\eta) = \int_0^\eta (\theta + N\phi) d\eta \quad (18)$$

Similarly, Eq. 3b goes over in

$$\theta'' + \frac{A}{B} \left( \frac{\dot{A}}{A} f\theta' - \frac{\dot{G}}{G} f'\theta \right) + D_f \phi'' = 0 \quad (19)$$

and Eq. 4b in

$$\frac{1}{Le} \phi'' + \frac{A}{B} \left( \frac{\dot{A}}{A} f\phi' - \frac{\dot{H}}{H} f'\phi \right) + S_r \theta'' = 0 \quad (20)$$

The dimensionless numbers occurring in the above equations were defined as

$$N = \frac{\beta_C km}{\beta_T D_m w}, \quad Le = \frac{\alpha_m}{D_m}, \quad D_f = \frac{k k_T m}{C_s C_p \alpha_m w}, \quad S_r = \frac{D_m^2 k_T w}{k T_m \alpha_m m} \quad (21)$$

It is worth noticing here that the sign of the buoyancy ratio  $N$ , Dufour and Soret numbers  $D_f$  and  $S_r$  depend on the directions of the prescribed wall fluxes, i.e. on  $\operatorname{sgn}(w)$  and  $\operatorname{sgn}(m)$  so that

$$\operatorname{sgn}(N) = \operatorname{sgn}(D_f) = \operatorname{sgn}(S_r) = \operatorname{sgn}(mw) \quad (22)$$

To be specific, we assume hereafter in this article that the heat flux is always directed from the wall to the fluid, i.e.  $w > 0$ . In this case, the signs of  $N$ ,  $D_f$ , and  $S_r$  coincide with the  $\operatorname{sgn}(m)$  of the mass flux  $q_m$ .

Equations 12, 15, and 16 give

$$G = \frac{wl}{k} \frac{q}{B}, \quad H = \frac{ml}{D_m} \frac{q}{B}, \quad A = \frac{q}{B^2} \quad (23)$$

where the reference length has been chosen as

$$l = \sqrt{\frac{\alpha_m v k}{g \beta_T w K}} \quad (24)$$

In this way

$$\begin{aligned} u &= u_0 \frac{q}{B} f'(\eta), \quad \eta = B(X)Y, \\ v &= -u_0 \frac{q}{B^2} \left[ \left( \frac{\dot{q}}{q} - 2 \frac{\dot{B}}{B} \right) f(\eta) + \frac{\dot{B}}{B} \eta f'(\eta) \right], \\ T &= T_\infty + \frac{wl}{k} \frac{q}{B} \theta(\eta), \quad C = C_\infty + \frac{ml}{D_m} \frac{q}{B} \phi(\eta) \end{aligned} \quad (25)$$

and Eqs. 19 and 20 become

$$\theta'' + \frac{q}{B^3} \left[ \left( \frac{\dot{q}}{q} - 2 \frac{\dot{B}}{B} \right) f\theta' - \left( \frac{\dot{q}}{q} - \frac{\dot{B}}{B} \right) f'\theta \right] + D_f \phi'' = 0 \quad (26)$$

$$\frac{1}{Le} \phi'' + \frac{q}{B^3} \left[ \left( \frac{\dot{q}}{q} - 2 \frac{\dot{B}}{B} \right) f\phi' - \left( \frac{\dot{q}}{q} - \frac{\dot{B}}{B} \right) f'\phi \right] + S_r \theta'' = 0 \quad (27)$$

The basic Eqs. 17, 26, and 27 are subjected to the boundary conditions specified under Eqs. 10, 11, and 13, i.e.

$$\begin{aligned} f(0) &= 0, & \theta'(0) &= -1, & \phi'(0) &= -1, \\ \theta(\infty) &= 0, & \phi(\infty) &= 0 \end{aligned} \quad (28)$$

### 3.2 Power-Law Variation of the Wall Fluxes: $q = X^p$

When the prescribed wall fluxes are of power-law functions of the wall coordinate  $X$ , Eqs. 26 and 27 can be reduced to ordinary differential equations only when  $B$  is a power-law function of  $X$ , too. In other words, the power-law similarity case of the present problem corresponds to

$$q = X^p, \quad B = B_0 X^b \quad (29)$$

where  $p$ ,  $b$ , and  $B_0$  are some dimensionless constants. In this case, Eqs. 26 and 27 yield

$$\theta'' + B_0^{-3} X^{p-3b-1} [(p-2b)f\theta' - (p-b)f'\theta] + D_f \phi'' = 0 \quad (30)$$

$$\frac{1}{Le} \phi'' + B_0^{-3} X^{p-3b-1} [(p-2b)f\phi' - (p-b)f'\phi] + S_r \theta'' = 0 \quad (31)$$

One sees that in this case the similarity reduction becomes possible only when  $b$  is related to  $p$  by the equation

$$b = \frac{p-1}{3} \quad (32)$$

Choosing  $B_0 = 3^{-1/3}$ , Eqs. 30 and 31 go over in

$$\theta'' + (p+2)f\theta' - (2p+1)f'\theta + D_f \phi'' = 0 \quad (33)$$

$$\frac{1}{Le} \phi'' + (p+2)f\phi' - (2p+1)f'\phi + S_r \theta'' = 0 \quad (34)$$

The velocity, temperature, and concentration fields are given in this case by the relationships

$$u = 3^{1/3} u_0 X^{\frac{2p+1}{3}} f'(\eta), \quad \eta = B(X) Y, \quad B(X) = 3^{-1/3} X^{\frac{p-1}{3}}, \quad (35)$$

$$v = -3^{-1/3} u_0 X^{\frac{p-1}{3}} [(p+2)f(\eta) + (p-1)\eta f'(\eta)],$$

$$T = T_\infty + 3^{1/3} \frac{wl}{k} X^{\frac{2p+1}{3}} \theta(\eta), \quad C = C_\infty + 3^{1/3} \frac{ml}{D_m} X^{\frac{2p+1}{3}} \phi(\eta),$$

$$f'(\eta) = \theta(\eta) + N\phi(\eta)$$

### 3.3 Exponential Variation of the Wall Fluxes: $q = e^{aX}$

Assuming that the prescribed wall fluxes are exponential functions of the coordinate  $X$ ,

$$q = e^{aX} \quad (36)$$

where  $a$  is a positive dimensionless parameter, Eqs. 26 and 27 can be reduced to ordinary differential equations only when  $B$  is also an exponential form, namely

$$B = B_0 e^{aX/3} \quad (37)$$

Indeed, choosing in this case  $B_0 = 3^{-1/3}$ , Eqs. 26 and 27 become

$$\theta'' + f\theta' - 2f'\theta + D_f\phi'' = 0 \quad (38)$$

$$\frac{1}{Le}\phi'' + f\phi' - 2f'\phi + S_r\theta'' = 0 \quad (39)$$

The velocity, temperature, and concentration fields are given in this case by the relationships

$$u = 3^{1/3}u_0 e^{2aX/3} f'(\eta), \quad \eta = 3^{-1/3}e^{aX/3}Y, \quad (40)$$

$$v = -3^{-1/3}u_0 a e^{aX/3} [f(\eta) + \eta f'(\eta)]$$

$$7T = T_\infty + 3^{1/3} \frac{wl}{k} e^{2aX/3} \theta(\eta), \quad C = C_\infty + 3^{1/3} \frac{ml}{D_m} e^{2aX/3} \phi(\eta),$$

$$f'(\eta) = \theta(\eta) + N\phi(\eta)$$

## 4 Flows with Thermosolutal Symmetry: $\phi(\eta) = \theta(\eta)$

### 4.1 Basic Requirements and Governing Equations

The present model admits a remarkable special case in which the dimensionless temperature and concentration fields  $\theta$  and  $\phi$  become coincident. In this case, Eq. 17 gives

$$\theta = \phi = \frac{f'}{1+N} \quad (41)$$

and Eqs. 26 and 27 imply that solutions with the thermosolutal symmetry,  $\theta = \phi$ , are only possible when

$$\Delta \equiv 1 + D_f - \left( S_r + \frac{1}{Le} \right) = 0 \quad \text{and} \quad N \neq -1 \quad (42)$$

When Eqs. 41 and 42 are satisfied, the dimensionless stream function  $f(\eta)$  is obtained as solution of the boundary value problem

$$(1 + D_f) f''' + \frac{q}{B^3} \left[ \left( \frac{\dot{q}}{q} - 2 \frac{\dot{B}}{B} \right) ff'' - \left( \frac{\dot{q}}{q} - \frac{\dot{B}}{B} \right) f'^2 \right] = 0 \quad (43)$$

$$f(0) = 0, \quad f''(0) = -(1+N), \quad f'(\infty) = 0 \quad (44)$$

after the similarity reduction of Eq. 43 in the power-law and exponential cases has been performed. In the former case (described in Sect. 3.2), Eq. 43 reduces to the equation

$$(1 + D_f) f''' + (p+2) ff'' - (2p+1) f'^2 = 0 \quad (45)$$

and in the exponential case (described in Sect. 3.3) to

$$(1 + D_f) f''' + ff'' - 2f'^2 = 0 \quad (46)$$

#### 4.2 Exact Solutions for Linear Wall Fluxes, $p = 1$

The boundary value problem (45), (44) admits for  $p = 1$ , the exact analytical solution

$$f(\eta) = \left[ \frac{(1+N)(1+D_f)^2}{9} \right]^{1/3} \left( 1 - \exp \left[ - \left( \frac{1+D_f}{3+3N} \right)^{-1/3} \eta \right] \right) \quad (47)$$

and using (41),

$$\theta(\eta) = \phi(\eta) = \frac{f'(\eta)}{1+N} = \left( \frac{1+D_f}{3+3N} \right)^{1/3} \exp \left[ - \left( \frac{1+D_f}{3+3N} \right)^{-1/3} \eta \right] \quad (48)$$

Thus, the wall values of  $\theta$ ,  $\phi$ , and  $f'$  are obtained as

$$\theta_0 = \phi_0 = \frac{f'(0)}{1+N} = \left( \frac{1+D_f}{3+3N} \right)^{1/3} = \left[ \frac{1+S_r Le}{3(1+N) Le} \right]^{1/3} \quad (49)$$

The asymptotic conditions and Eq. 42 require in this case that

$$\operatorname{sgn}(1+N) = \operatorname{sgn}(1+D_f) = \operatorname{sgn} \left( \frac{1}{Le} + S_r \right) \quad (50)$$

#### 4.3 Exact Solutions for Inverse Linear Wall Fluxes, $p = -1$

Equation 45 reduces for  $p = -1$  to

$$(1+D_f) f''' + ff'' + f'^2 = 0 \quad (51)$$

and after two successive integrations leads to the equations

$$(1+D_f) f'' + ff' = C_1 \quad (52)$$

$$(1+D_f) f' + \frac{1}{2} f^2 = C_1 \eta + C_2 \quad (53)$$

where  $C_1$  and  $C_2$  are constants of integration. Bearing in mind the wall conditions (44), one easily obtains

$$C_1 = -(1+N)(1+D_f), \quad C_2 = (1+D_f) f'(0) \quad (54)$$

Furthermore, the asymptotic condition (44) implies

$$C_1 = \lim_{\eta \rightarrow \infty} (ff') = \frac{1}{2} \lim_{\eta \rightarrow \infty} \left( \frac{f^2}{\eta} \right) \quad (55)$$

These equations have two important consequences. Firstly, they imply that the problem admits real solutions only when  $C_1 > 0$  which, on account of Eqs. (54) and (42) requires

$$\operatorname{sgn}(1+N) = -\operatorname{sgn}(1+D_f) = -\operatorname{sgn} \left( \frac{1}{Le} + S_r \right) \quad (56)$$

The second consequence of Eqs. 55 is the algebraic asymptotic behavior of  $f$  and  $f'$ , namely

$$f \sim \pm \sqrt{2C_1 \eta}, \quad f' \sim \pm \sqrt{\frac{C_1}{2\eta}} \text{ as } \eta \rightarrow \infty \quad (57)$$

The corresponding solution of the Riccati equation (53) can be given in terms of the Airy function  $Ai(z)$  as

$$f(\eta) = [4(1 + D_f)C_1]^{1/3} \frac{Ai'(z)}{Ai(z)} \quad (58)$$

where

$$z = \left[ \frac{C_1}{2(1 + D_f)^2} \right]^{1/3} \eta + z_0 \quad (59)$$

and  $Ai'(z)$  is the derivative of  $Ai(z)$  with respect to  $z$  (for the properties of the Airy functions, see e.g. Abramowitz and Stegun 1972, Chap. 10.4). The constant  $z_0$  is determined from the boundary condition  $f(0) = 0$  as the first zero of  $Ai'(z)$  which is  $z_0 = -1.018792971$ . In this way

$$\theta(\eta) = \phi(\eta) = \frac{f'(\eta)}{1 + N} = \frac{1}{1 + N} \left[ f'(0) + \frac{C_1}{1 + D_f} \eta - \frac{1}{2(1 + D_f)} f^2 \right] \quad (60)$$

where  $f'(0)$  is given by

$$f'(0) = z_0 \left( \frac{2C_1^2}{1 + D_f} \right)^{1/3} \quad (61)$$

Thus, the wall values of  $\theta$  and  $\phi$  are obtained as

$$\theta_0 = \phi_0 = z_0 \left[ \frac{2(1 + D_f)}{1 + N} \right]^{1/3} = |z_0| \left| \frac{2(1 + D_f)}{1 + N} \right|^{1/3} \quad (62)$$

In this way,

$$\theta(\eta) = \phi(\eta) = \theta_0 - \eta + \left( \frac{2(1 + D_f)^2}{C_1} \right)^{1/3} \left[ \frac{Ai'(z)}{Ai(z)} \right]^2 \quad (63)$$

Bearing in mind Eq. 62 and  $z_0 = -1.018792971$ , we further obtain

$$\theta_0 = \phi_0 = 1.28359871 \left| \frac{1 + D_f}{1 + N} \right|^{1/3} \quad (64)$$

where, in addition to Eq. 56, also Eq. 42 holds.

#### 4.4 Exact Solutions for Inverse Quadratic Wall Fluxes, $p = -2$

According to Eqs. 35, for the velocity, temperature, and concentration fields of the symmetric thermosolutal flows depend only on the first derivative of the similar stream function  $f'(\eta)$ . The corresponding boundary value problem (45), (44) admits for  $f'(\eta)$  the exact solution

$$f'(\eta) = -2(1 + D_f) \left[ \eta - \left( \frac{4 + 4D_f}{1 + N} \right)^{1/3} \right]^{-2} \quad (65)$$

The non-singularity condition in this case is  $\operatorname{sgn}(1+N) = -\operatorname{sgn}(1+D_f)$  which in turn coincides with Eq. 56. Thus, the temperature and concentration fields are obtained as

$$\theta(\eta) = \phi(\eta) = 2 \left| \frac{1+D_f}{1+N} \right| \left[ \left| \frac{4+4D_f}{1+N} \right|^{1/3} + \eta \right]^{-2} \quad (66)$$

The asymptotic decay is algebraic also in this case,  $\theta(\eta) \rightarrow 0$  as  $1/\eta^2$  when  $\eta \rightarrow \infty$ , but much faster than in the inverse linear case discussed in Sect. 4.3. Nevertheless, the surface temperature and concentration

$$\theta_0 = \phi_0 = 2^{-1/3} \left| \frac{1+D_f}{1+N} \right|^{1/3} \quad (67)$$

differ from the values given by Eq. 64 by a constant factor only.

#### 4.5 Scaling Transformations

Changing from the variables  $(\eta, f)$  to the new ones  $(\xi, F)$  by the scaling transformations

$$f(\eta) = (1+D_f) \left| \frac{1+N}{1+D_f} \right|^{1/3} F(\xi), \eta = \left| \frac{1+D_f}{1+N} \right|^{1/3} \xi \quad (68)$$

the Dufour number can be removed from the governing Eqs. 45 and 46 which reduce to

$$\ddot{F} + (p+2)F\ddot{F} - (2p+1)\dot{F}^2 = 0 \quad (69)$$

$$\ddot{F} + FF\ddot{F} - 2\dot{F}^2 = 0 \quad (70)$$

where the dots denote differentiations with respect to  $\xi$ . The boundary conditions (44) become

$$F(0) = 0, \ddot{F}(0) = -s, \dot{F}(\infty) = 0 \quad (71)$$

where

$$s = \operatorname{sgn}(1+D_f) \operatorname{sgn}(1+N) \quad (72)$$

Similarly, one obtains

$$f'(\eta) = (1+D_f) \left| \frac{1+N}{1+D_f} \right|^{2/3} \dot{F}(\xi), \xi = \left| \frac{1+N}{1+D_f} \right|^{1/3} \eta \quad (73)$$

$$\theta(\eta) = \phi(\eta) = s \left| \frac{1+D_f}{1+N} \right|^{1/3} \dot{F}(\xi) \quad (74)$$

$$\theta_0 = \phi_0 = s \left| \frac{1+D_f}{1+N} \right|^{1/3} \dot{F}(0) \quad (75)$$

The advantage of the above scaling transformations is that after the values of  $p$  and  $s$  are specified, the “missing initial value”  $\dot{F}(0)$  does not depend on the parameters  $N$  and  $D_f$  at all. Thus, the numerical solutions for  $\dot{F}(\xi)$  of the problems (69), (71) and (70), (71) yield all the quantities of interest via Eqs. 73–75 explicitly.

## 5 Discussion

The velocity, temperature, and concentration solutions of the boundary value problem (1–5) considered in the present investigation are given in the case of power-law and exponential similarity by Eqs. 35 and 40, respectively. Bearing in mind that the surface fluxes  $q_w(x) = wq(X)$  and  $q_m(x) = mq(X)$  are prescribed, the quantities of the main engineering interest are the surface temperature and concentrations distributions  $T(x, 0) \equiv T_w(x)$  and  $C(x, 0) \equiv C_w(x)$ , respectively. These quantities are obtained from the wall values  $\theta_0 = \theta(0)$  and  $\phi_0 = \phi(0)$  of respective self-similar temperature and concentration solutions  $\theta(\eta)$  and  $\phi(\eta)$ . In order to reduce the parametric complexity of the analysis, we still assume that the heat flux is always positive ( $w > 0$ ) so that the general relationship (22) for the signs of the basic transport parameters reduces to

$$\operatorname{sgn}(N) = \operatorname{sgn}(D_f) = \operatorname{sgn}(S_r) = \operatorname{sgn}(m) \quad (76)$$

The main goal of the present section is a detailed discussion of the basic temperature and concentration characteristics of the flows with thermosolutal symmetry,  $\theta(\eta) = \phi(\eta) = f'(\eta)/(1+N)$ , for which the additional restrictions (42) hold. We mention that the value  $N = -1$ , excluded by Eqs. 42, corresponds to the physical situation in which the thermal and solutal buoyancy forces compensate each other. Since in the present model the buoyancy is the only driving force of the flow, the value  $N = -1$  is associated with the (trivial) static equilibrium state of the system. This is the reason why the value  $N = -1$  has been excluded. It is also worth noticing here that the vanishing value of the buoyancy ratio  $N$  corresponds to the physical situation in which the solutal buoyancy is negligible with respect to the thermal one ( $|m| \ll |w|$ ).

### 5.1 The Exactly Solvable Cases $p = 1$ , $p = -1$ , and $p = -2$

For linear wall fluxes ( $p = 1$ ), the surface values of the self-similar temperature and concentration fields are given by Eq. 49 which require that the transport coefficients satisfy, in addition to Eqs. 68 the restrictions (50). Taking into account these circumstances in Fig. 1a, the values  $\theta_0 = \phi_0$  have been plotted as functions of  $N$  for three selected values of the Dufour number. In Fig. 1b, based on Eq. 42, the corresponding variation ranges of the Soret number as function of the Lewis number are shown. The dot on the green curve of Fig. 1b corresponds to the situation in which both of the cross-diffusion effects can be neglected,  $D_f = S_r = 0$ . In this case, the unity value  $Le = 1$  of the Lewis number is required. The other points of the green curves of Fig. 1 describe the flows with a negligible Dufour number (negligible diffusion-thermo effect) compared to Soret number (thermodiffusion effect). The dots on the red and blue curves of Fig. 1b correspond to the opposite situation,  $S_r = 0, D_f \neq 0$ . The other points of the red and blue curves of Fig. 1b illustrate the contribution of the cross-diffusion effects compared to the point on the green curve corresponding to  $D_f = S_r = 0$ . The temperature and concentration profiles  $\theta(\eta) = \phi(\eta)$  associated with the parameter values of Fig. 1, according to Eq. 48, are simple exponential functions decaying from the corresponding surface values (49) toward zero as  $\eta \rightarrow \infty$ .

In contrast to these exponentially decaying profiles, the Airy function profiles corresponding to the inverse linear wall fluxes ( $p = -1$ ) shown in Fig. 2a, are algebraically decaying functions. Specifically, in the latter case  $\theta, \phi$ , and  $f' \rightarrow 0$  as  $\eta^{-1/2}$  when  $\eta \rightarrow \infty$ . This very slow algebraic decay is the reason why in the case  $p = -1$  the numerical approach, in contrast to the analytical one, encounters serious convergence problems for large values of

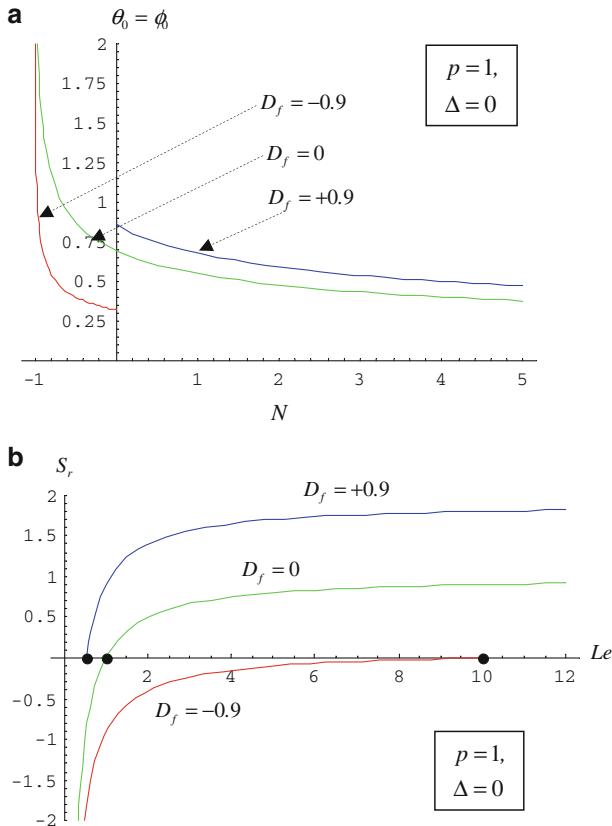


**Fig. 1** **a** Plots of the wall temperature  $\theta_0$  (and concentration  $\phi_0$ ) for symmetric thermosolutal flows ( $\Delta = 0$ ) and linear wall fluxes ( $p = 1$ ) as functions of the buoyancy ratio  $N$  for the indicated values of the Dufour number. **b** Plots of the Soret number  $S_r$  as a function of the Lewis number  $Le$  for symmetric thermosolutal flows ( $\Delta = 0$ ) with linear wall fluxes ( $p = 1$ ) for the values of the Dufour number considered in Fig. 2a. The dots correspond to the values  $Le = 1/(1+D_f)$  where in the respective Eq. (42)  $S_r = 0$

$\eta$ . In Fig. 2b, based on Eqs. 42 and 56, the variation ranges of the Soret number as function of the Lewis number are shown for the values of the Dufour number considered in Fig. 2a. In the case of inverse quadratic fluxes  $p = -2$ , the qualitative features of the solution are similar to those corresponding to  $p = -1$ . The physical interpretation of the dots and curves seen in Fig. 2b is similar to that described in connection with Fig. 1b.

## 5.2 Wall Fluxes with: $p \geq 0$

In the case of constant ( $p = 0$ ) and power-law heat and mass fluxes with  $p > 0$ , it is convenient to conduct the discussion of the symmetric thermosolutal flows ( $\Delta = 0$ ) on the basis of the rescaled boundary value problem (69), (71), and (72). In this context, the quantity of the main computational interest (for specified values of  $p$  and  $s$ ) is the corresponding “initial value”  $\dot{F}(0; p)$ . This quantity can easily be determined with the aid of the shooting method. The values of  $\dot{F}(0; p)$  determined in this way for  $s = +1$  and some selected values of  $p \geq 0$  have been collected in Table 1 and represented in Fig. 3 as functions of  $p$ .

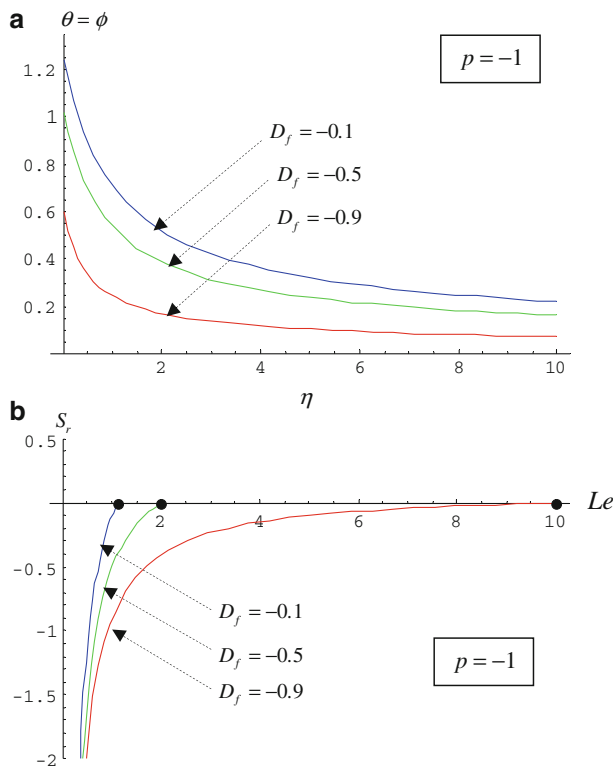


**Fig. 2** **a** Airy function profiles of the dimensionless temperature and concentration profiles of the symmetric thermosolutal flows with inverse linear wall fluxes ( $p = -1$ ) for the buoyancy ratio  $N = -2$  and the indicated values of the Dufour number. **b** Plots of the Soret number  $S_r$  as a function of the Lewis number  $Le$  for symmetric thermosolutal flows with inverse linear wall fluxes ( $p = -1$ ) for the values of the Dufour number considered in Fig. 2a. The dots correspond to the values  $Le = 1/(1 + D_f)$  where in the respective Eq. 42

$S_r = 0$

**Table 1** The values of  $\dot{F}(0; p)$  in the case of symmetric thermosolutal flows ( $\Delta = 0$ ) for  $s = +1$  and the indicated values of the power-law exponent  $p$

$p$	0	0.5	1	2	3	5	6.5	8	10
$\dot{F}(0; p)$	0.8987	0.7706	0.6934	0.5997	0.5422	0.4712	0.4365	0.4102	0.3832

In Fig. 4, the wall temperature  $\theta_0$  and concentration  $\phi_0$  for symmetric thermosolutal flows and constant wall fluxes have been plotted along the buoyancy ratio  $N$  for the indicated values of the Dufour number. Another plot describing the thermosolutal symmetry is shown in Fig. 5 for  $N = 1$  and three different values of the Dufour number. Wall temperature and concentration reduce when the power-law index  $p$  increases, while the Dufour effect produces smaller Nusselt numbers ( $1/\theta_0$ ) or Sherwood numbers ( $1/\phi_0$ ).

### 5.3 Comparison of the Symmetric and Non-Symmetric Flows

In this subsection, we are interested to gain some insight on what happens when the heat and mass transfer process deviates from symmetric to non-symmetric thermo-solutal conditions.

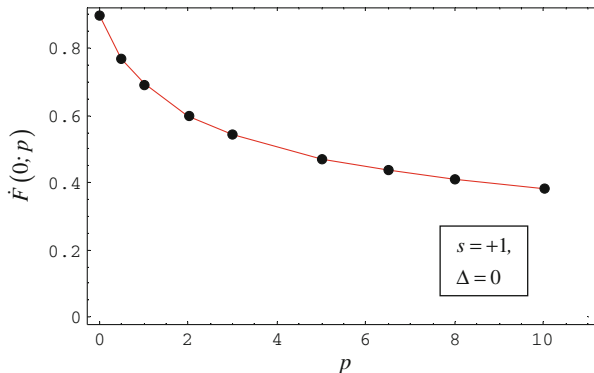


**Fig. 3** The values of  $\dot{F}(0; p)$  collected in Table 1 and plotted as function of  $p$

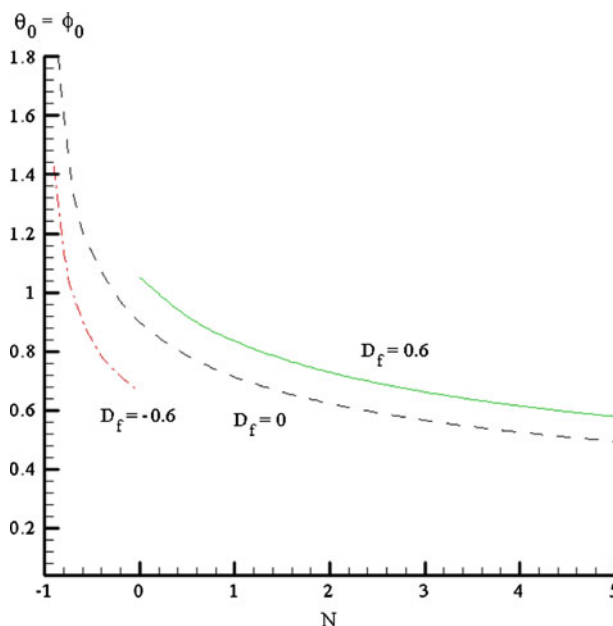


**Fig. 4** Wall temperature  $\theta_0$  (and wall concentration  $\phi_0$ ) variation with  $N$ , when  $p = 0$ , for three different values of the Dufour number

Due to the large number of parameters involved in the problem, we concentrate on two combinations of  $D_f$  and  $S_r$  characterized by the mutual prevalence between them, by keeping  $N = 1$ , in the case of constant wall heat and mass fluxes. The reported results, discussed in some detail, focus on the wall temperatures and concentrations, whose reciprocal values are of the Nusselt and Sherwood numbers, respectively

The curves plotted in Figs. 6 and 7 are obtained by numerically solving Eqs. 33–34 subject to (28). The intersection points of the curves  $\theta_0$  and  $\phi_0$  are marked by circles and correspond to the flows with thermosolutal symmetry ( $\Delta = 0$ ). On the other hand, for  $\Delta = 0$ , it is possible to compute  $\theta_0 = \phi_0$  by solving the rescaled boundary value problem (69), (71), (72), and using then (75). This is of course not only an alternative, but also of help in guessing the

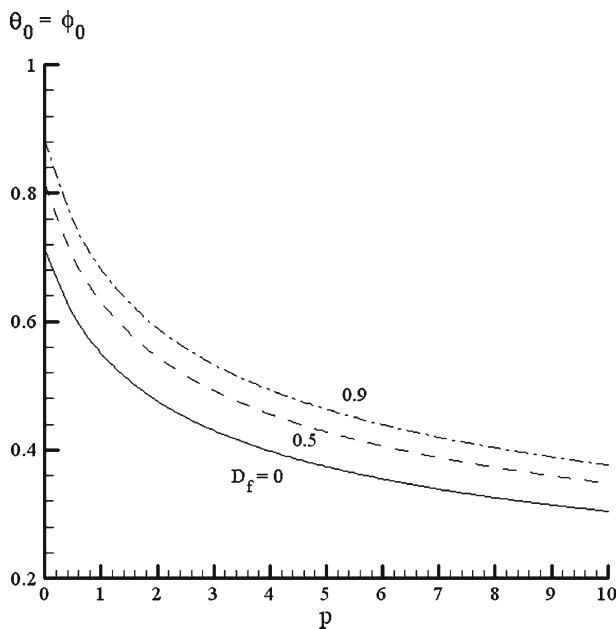


**Fig. 5** Wall temperature  $\theta_0$  (and wall concentration  $\phi_0$ ) variation with  $p \geq 0$  for  $N = 1$ , and three different values of the Dufour number

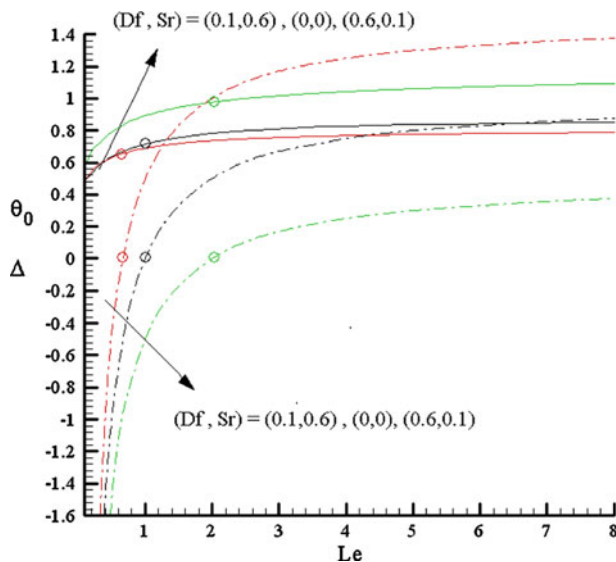


**Fig. 6** Plots of the wall temperature  $\theta_0$  (solid lines) and  $\Delta$  (dash dot) versus Lewis number, for constant wall fluxes ( $p = 0$ ), and buoyancy ratio  $N = 1$ . The circles correspond to the symmetric case,  $\Delta = 0$

missing slopes for the more complex problem (33–34) and (28). The variation of  $\Delta$  with the Lewis number was also included in both figures.

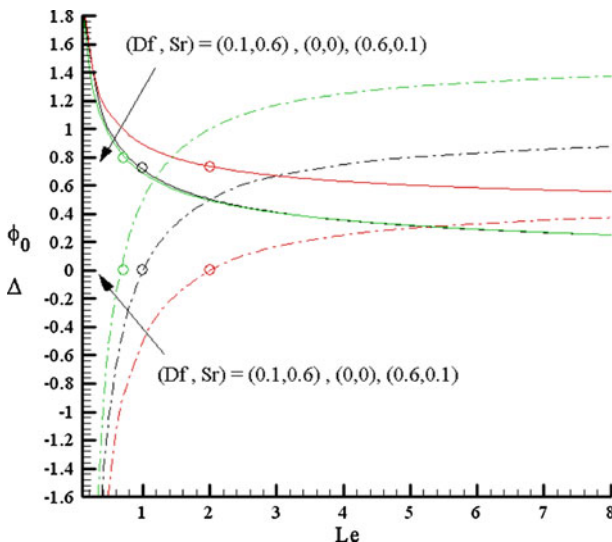


**Fig. 7** Plots of the wall concentration  $\phi_0$  (solid lines) and  $\Delta$  (dash dot) versus Lewis number, for constant wall fluxes ( $p = 0$ ), and buoyancy ratio  $N = 1$ . The circles correspond to the symmetric case,  $\Delta = 0$

An overall inspection of these figures shows an opposite behavior of the wall temperature and concentration with Lewis number: when  $Le$  increases (i.e. when heat diffusion becomes prevalent over mass diffusion),  $\theta_0$  slightly increases, while the decrease of  $\phi_0$  is more pronounced. The smooth transition through the state of thermosolutal symmetry is clearly seen in both Figs. 6 and 7.

It is not surprisingly to notice the stronger impact of the combination ( $D_f > S_r$ ) on the wall temperature, in comparison with the case  $D_f < S_r$ . Nusselt number decreases in the transition ( $D_f < S_r$ ), ( $D_f = S_r = 0$ ), ( $D_f > S_r$ ), at fixed values of the other parameters ( $N$  and  $Le$ ).

For the wall concentration, the departure from thermosolutal symmetry is significant when  $D_f < S_r$ . One remarks the increase of the Sherwood number in the transition ( $D_f < S_r$ ), ( $D_f = S_r = 0$ ), ( $D_f > S_r$ ). It is somehow expectable to get a stronger influence of a larger Soret number on the mass transfer, on physical and also on mathematical reasons. Incidentally, the values of  $\phi_0$  are very close to each other in the cases ( $D_f = 0.6, S_r = 0.1$ ) and ( $D_f = 0, S_r = 0$ ).

## 6 Conclusions

The double-diffusive natural convection past a vertical plate embedded in a fluid-saturated porous medium was considered in the boundary-layer and Boussinesq approximation, assuming that the Soret–Dufour cross-diffusion effects are significant. The heat and mass fluxes on the plate were prescribed as functions of the surface streamwise coordinate. Once the general similarity reduction of the problem was obtained for both power-law and exponential variation of the wall fluxes, we decided to go into details for the former case. The basic remark in this regard is the resemblance of Eqs. 33–34 and 38–39 in the general case and of (45) and (46) in the case of thermosolutal symmetry. Although extensive computations have

been also performed for the exponential case, we do not present here numerical results for this case, for sake of space saving, since they are qualitatively similar to those obtained for power-law variations of the heat and mass fluxes.

Our main interest was directed on the self-similar flows with thermosolutal symmetry, when the similar temperature and concentration fields become coincident. In these cases, exact analytical solutions were obtained in the following cases of heat and mass power-law fluxes: linear ( $p = 1$ ), inverse linear ( $p = -1$ ), and inverse quadratic ( $p = -2$ ). In contrast to exponentially decaying profiles obtained in the linear case, we found for  $p = -1$  and  $p = -2$  an algebraically decaying behavior of the solution. Moreover, for power-law heat and mass fluxes, we have been able to find appropriate scaling transformations allowing the reduction of the boundary value problems to such ones no more dependent on the physical (dimensionless) parameters. This considerably reduces the efforts of computation.

For flows without thermosolutal symmetry, a numerical approach has been used for both cases of power-law and exponential variation of the heat and mass fluxes. The analysis of the influence of departure from thermosolutal symmetry due to the Soret and Dufour effects was performed specifically when  $p = 0$ , and revealed that Nusselt number is more affected than Sherwood number in the cases with ( $D_f > S_r$ ), while the situation reverses when ( $D_f < S_r$ ). Although these results have been obtained for constant wall fluxes (easier to be implemented in practical applications), the trends will be the same for any  $p > 0$ .

## References

- Abramowitz, M., Stegun, I.A.: *Handbook of Mathematical Functions*. Dover, New York (1972)
- Afify, A.: Effects of temperature-dependent viscosity with Soret and Dufour numbers on non-Darcy MHD free convective heat and mass transfer past a vertical surface embedded in a porous medium. *Transp. Porous Media* **66**, 391–401 (2007a)
- Afify, A.: Effects of thermal-diffusion and diffusion-thermo on non-Darcy MHD free convective heat and mass transfer past a vertical isothermal surface embedded in a porous medium with thermal dispersion and temperature-dependent viscosity. *Appl. Math. Model.* **31**, 1621–1634 (2007b)
- Anghel, M., Takhar, H.S., Pop, I.: Dufour and Soret effects on free convection boundary-layer over a vertical surface embedded in a porous medium. *Studia Universitatis Babes-Bolyai Mathematica* **XLV** **11**(22), 11–22 (2000)
- Benano-Melly, L.B., Caltagirone, J.P., Faissat, B., Montel, F., Costeseque, P.: Modelling Soret coefficient measurement experiments in porous media considering thermal and solutal convection. *Int. J. Heat Mass Transf.* **44**, 1285–1297 (2001)
- Chamka, A.J., Ben-Nakhi, A.: MHD mixed convection–radiation interaction along a permeable surface immersed in a porous medium in the presence of Soret and Dufour’s effects. *Heat Mass Transf.* **44**, 845–856 (2008)
- Cheng, C.-Y.: Soret and Dufour effects on natural convection heat and mass transfer from a vertical cone in a porous medium. *Int. Commun. Heat Mass Transf.* **36**, 1020–1024 (2009)
- Eckert, E.R.G., Drake, R.M.: *Analysis of heat and mass transfer*. McGraw-Hill, New York (1972)
- Gaikwad, S.N., Malashetty, M.S., Rama Prasad, K.L.: Linear and non-linear double diffusive convection in a fluid-saturated anisotropic porous layer with cross-diffusion effects. *Transp. Porous Media* **80**, 537–560 (2009)
- Johnson, C.H., Cheng, P.: Possible similarity solutions for free convection boundary-layers adjacent to flat plates in porous media. *Int. J. Heat Mass Transf.* **21**, 709–718 (1978)
- Kafoussias, N.G., Williams, E.W.: Thermal-diffusion and diffusion-thermo effects on mixed free-forced convective and mass transfer boundary layer flow with temperature dependent viscosity. *Int. J. Eng. Sci.* **33**, 1369–1384 (1995)
- Lakshmi Narayana, P.A., Murthy, P.V.S.N.: Soret and Dufour effects in a doubly stratified Darcy porous medium. *J. Porous Media* **10**, 613–624 (2007)
- Lakshmi Narayana, P.A., Murthy, P.V.S.N.: Soret and Dufour effects on free convection heat and mass transfer from a horizontal flat plate in a Darcy porous medium. *J. Heat Transf. Trans. ASME* **130**, 104504–11045045 (2008)

- Li, M., Tia, Y., Zhai, Y.: Soret and Dufour effects in strongly endothermic chemical reaction system of porous media. *Trans. Nonferrous Met. Soc. China* **16**, 1200–1204 (2008)
- Mojtabi, A., Charrier-Mojtabi, M.C.: Double-diffusive convection in porous media. In: Vafai, K. (ed.) *Handbook of Porous Media*, pp. 559–603. Marcel Dekker, New York (2000)
- Nield, D.A., Bejan, A.: *Convection in Porous Media*, 3rd edn. Springer, New York (2006)
- Partha, M.K., Murth, P.V.S.N., Raja Sekhar, G.P.: Soret and Dufour effects in a non-Darcy porous medium. *J. Heat Transf. Trans. ASME* **128**, 605–610 (2006)
- Platten, J.K., Legros, J.C.: *Convection in liquids*. Springer, New York (1984)
- Postelnicu, A.: Influence of a magnetic field on heat and mass transfer by natural convection from vertical surfaces in porous media considering Soret and Dufour effects. *Int. J. Heat Mass Transf.* **47**, 1467–1472 (2004)
- Postelnicu, A.: Influence of chemical reaction on heat and mass transfer by natural convection from vertical surfaces in porous media considering Soret and Dufour effects. *Heat Mass Transf.* **43**, 595–602 (2007)
- Postelnicu, A.: Heat and mass transfer by natural convection at a stagnation point in a porous medium considering Soret and Dufour effects. *Heat Mass Transf.* **46**, 831–840 (2010)
- Rathish Kumar, B.V., Krishna Murthy, S.V.S.S.N.V.G.: Soret and Dufour effects on double-diffusive free convection from a corrugated vertical surface in a non-Darcy porous medium. *Transp. Porous Media* (2010). doi:[10.1007/s11242-010-9549-0](https://doi.org/10.1007/s11242-010-9549-0) (online)
- Saghir, M.Z., Jiang, C.G., Chacia, M., Yan, Y., Khawaja, M., Pan, S.: Thermodiffusion in porous media. In: Ingham, D., Pop , I. (eds.) *Transport Phenomena in Porous Media III*, Chap. 9, Pergamon, Oxford (2005)
- Soret, C.: Influence de la température sur la distribution des sels dans leurs solutions. *C.R. Acad. Sci. Paris* **91**, 289–291 (1880)
- Tsai, R., Huang, J.S.: Heat and mass transfer for Soret and Dufour's effects on Hiemenz flow through porous medium onto a stretching surface. *Int. J. Heat Mass Transf.* **52**, 2399–2406 (2009a)
- Tsai, R., Huang, J.S.: Numerical study of Soret and Dufour effects on heat and mass transfer from natural convection flow over a vertical porous medium with variable wall heat fluxes. *Comp. Mat. Sci.* **47**, 23–30 (2009b)